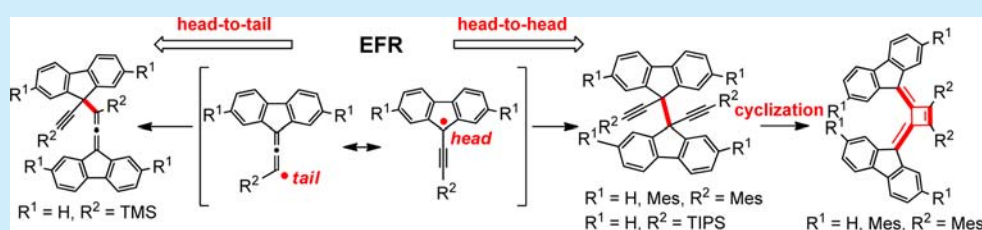


9-Ethynylfluorenyl Radicals: Regioselective Dimerization and Post Ring-Cyclization Reactions

Shuhai Qiu,[†] Youyu Zhang,[‡] Xiaobo Huang,[§] Lipiao Bao,^{||} Youhua Hong,[†] Zebing Zeng,^{*,†,||} and Jishan Wu[⊥][†]State Key Laboratory of Chemo/Biosensing and Chemometrics, College of Chemistry and Chemical Engineering, Hunan University, Changsha 410082, P. R. China[‡]Key Laboratory of Chemical Biology and Traditional Chinese Medicine Research (Ministry of Education), College of Chemistry and Chemical Engineering, Hunan Normal University, Changsha 410081, P. R. China[§]College of Chemistry and Materials Engineering, Wenzhou University, Wenzhou 325035, P. R. China^{||}State Key Laboratory of Materials Processing and Die & Mold Technology, School of Materials Science and Engineering, Huazhong University of Science and Technology (HUST), Wuhan 430074, P. R. China[⊥]Department of Chemistry, National University of Singapore, 3 Science Drive 3, 117543 Singapore

S Supporting Information



ABSTRACT: 9-Ethynylfluorenyl radical derivatives were readily prepared in situ and underwent simultaneous intermolecular coupling reactions. Interestingly, the dimerization process took place in either a head-to-tail or a head-to-head mode between the acetylenic or the allenic resonance forms dependent on the terminal substituents, which could be well explained by their different spin distribution and steric hindrance effects. The structures of the products were confirmed by X-ray crystallographic and other spectroscopic analyses. It was also found that the newly generated dipropynyl dimers underwent a rearrangement and ring-cyclization reaction at room temperature, eventually giving unique difluorenylidene cyclobutene derivatives.

Carbon-centered radicals have attracted much attention due to their important role as reactive intermediates in constructing complicated polycyclic aromatic hydrocarbons (PAHs) and their potential applications as organic magnetic materials.¹ The key challenge is to stabilize the radical, which is usually highly reactive toward other substances or environmental media such as oxygen and water. The fulvenallenyl radical (Figure 1a, left), usually produced by flash pyrolysis of hydrocarbons,² has been investigated as the major intermediate for the formation of PAHs.³ Both the cyclopentadienyl and the allenyl resonance forms contribute significantly to its ground-state geometry, and there are high spin densities at both the *ipso*-carbon in the five-membered ring and the terminal allenyl carbon. The high reactivity of the fulvenallenyl radical led to unpredictable products in the subsequent reactions. We became interested in the doubly benzannulated fulvenallenyl radical, the so-called 9-ethylfluorenyl radical (EFR), which is expected to be much more stable due to the kinetic blocking and thermodynamic delocalization of the unpaired electron (Figure 1a, right).⁴

Computational models suggested that the fulvenallenyl radical potentially produced PAHs in sooting aromatic flames



Figure 1. (a) Resonance structures of the fulvenallenyl radicals (left) and 9-ethylfluorenyl radical EFR (right). (b) Possible dimer structures D1–D3 via radical–radical coupling reaction.

by self-reaction and cross-reactions,^{3a,b,5} but direct experimental proof was lacking. In the case of EFR, the highest spin density is thought to localize at the 9-fluorenyl position (head, carbon “d”) and the terminal allenyl site (tail, carbon “e”) based a simple resonance form analysis (Figure 1a, right), and thus,

Received: September 27, 2016

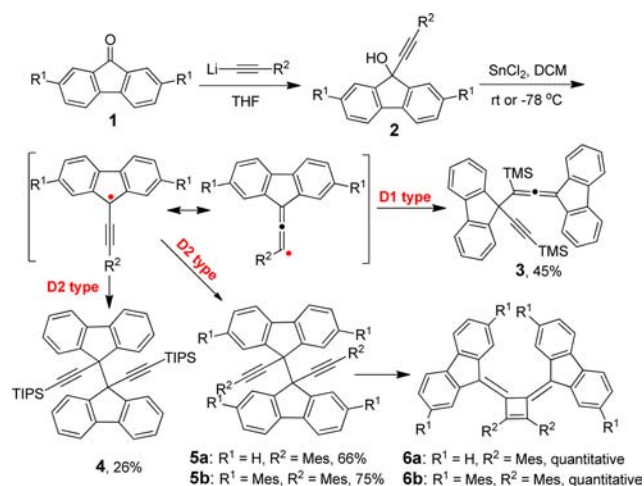
Published: November 18, 2016



intermolecular radical–radical coupling could take place to give dimers with three possible linkage modes: head-to-tail (D1), head-to-head (D2), and tail-to-tail (D3) (Figure 1b). In this paper, we demonstrate the regioselective dimerization of the in situ generated EFR derivatives with different substitutions at the terminal alkyne and the subsequent interesting rearrangement and ring-cyclization reaction, which eventually led to the formation of a unique difluorenylidene cyclobutene structure.

The synthetic route used to generate EFR radicals with different substituents (TMS, trimethylsilyl; TIPS, triisopropylsilyl; Mes, mesityl) is shown in Scheme 1. Addition of the

Scheme 1. Synthesis of the EFR Derivatives and the Subsequent Dimerization and Ring-Cyclization Reactions



lithiated alkyne reagents⁶ to the commercially available 9-fluorenone- or the 2,7-bismesityl-substituted 9-fluorenone **1** afforded the corresponding alcohol precursors **2**. A characteristic deep color indicative of EFR formation appeared in time periods from several minutes to 1 h after treatment of the hydroxyl precursors **2** with SnCl₂ in dry dichloromethane (DCM) at room temperature, the as-generated radicals were further converted into the dimers **3** (R¹ = H, R² = TMS), **4** (R¹ = H, R² = TIPS), or **5** (R¹ = H/Mes, R² = Mes) within 30 min, and the color of the solution became light over the time.

Compound **3** was obtained as a white crystalline substance showing adequate stability at ambient temperature, consistent with previously reported propargyl allene compounds,⁷ when the reduction of the TMS-substituted alcohol precursor **2** was conducted at room temperature for 3 h. Compound **3** can be also synthesized at low temperature (−20 to −78 °C). The clearly correlated ¹³C NMR resonances for the propargyl and allenyl functional groups (Figure S12) suggest that the dimerization took place in a head-to-tail mode (D1 type), and the structure of **3** was further confirmed by X-ray crystallographic analysis (vide infra). The UV–vis absorption spectrum of **3** in DCM displays intense absorbance in the range of 250–360 nm, with the lowest energy absorption maximum (λ_{max}) at 324 nm (Figure 2).

Treatment of larger bulky TIPS-substituted hydroxyl precursor **2** with reductant SnCl₂ at −78 °C or room temperature gave **4** as a white powder in 26% isolated yield. Because of the large steric hindrance, the dimerization of the TIPS-protected EFR proceeded less efficiently. Compound **4** shows a slightly blue-shifted absorption spectrum compared to **3**, with λ_{max} at 322 nm (Figure 2). No resonance peak appears

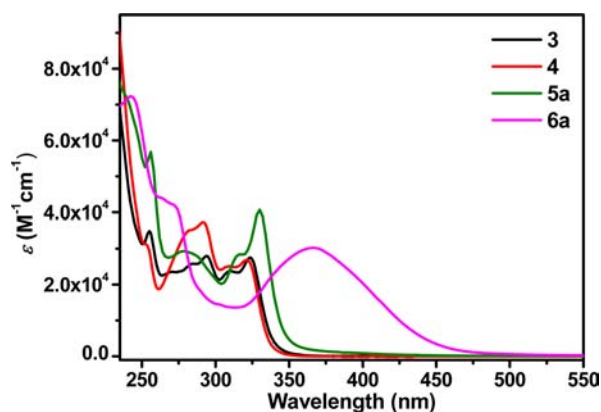


Figure 2. UV–vis absorption spectra of **3**, **4**, **5a**, and **6a** in DCM.

above 190 ppm in the ¹³C NMR spectrum of **4** (Figure S14), indicating that it does not possess an allenic unit (a ¹³C NMR peak at 205 ppm was observed for **3**). The direct head-to-head linkage (D2 type) was further confirmed by X-ray crystallographic analysis (vide infra).

In contrast to **4**, reduction of Mes-substituted precursors **2** at room temperature or −78 °C finally gave a yellow solid **6a** (R¹ = H, R² = Mes)/**6b** (R¹ = Mes, R² = Mes) within 2 h. The main absorption bands of **6a/6b** are red-shifted to λ_{max} = 365 and 372 nm, respectively (Figure 2 and Figure S1), indicating a relatively longer conjugation length formed in comparison with the former dimers. Interestingly, a white intermediate **5a** (R¹ = H, R² = Mes) with the main absorption band λ_{max} at 330 nm was isolated when the reaction was conducted at −78 °C before formation of **6a**. This white compound was quantitatively converted into the yellow **6a** in solution at room temperature, suggesting that **5a** is an intermediate state. However, compound **5a** was found to have poor solubility. Therefore, two mesityl groups were attached onto the 2,7-positions of the parent fluorene unit to improve both solubility and stability. A white compound **5b** (R¹ = Mes, R² = Mes) with good solubility was then isolated, and it was slowly converted into a yellowish compound **6b** in solution over several days. It exhibits a similar absorption spectrum to **4**, with λ_{max} at 265 nm (Figure 2).

Single crystals suitable for X-ray crystallographic analysis (Figure 3) were obtained for **3**, **4**, **5b**, and **6a,b** via slow

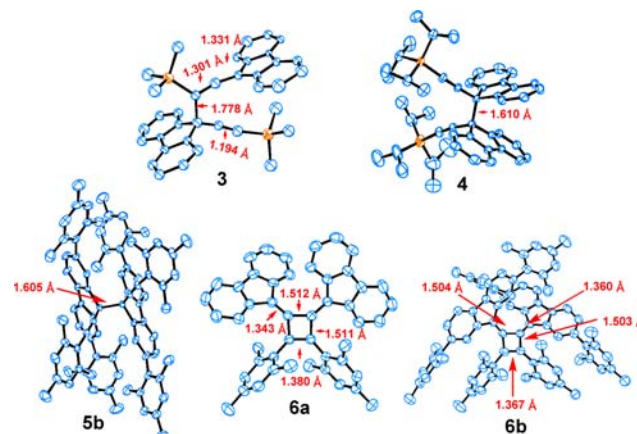
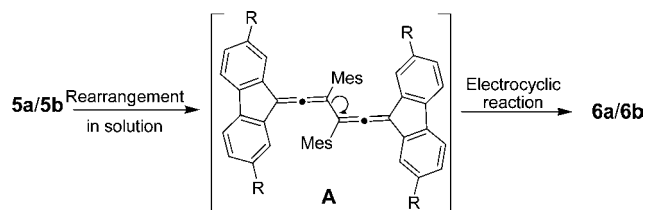


Figure 3. X-ray crystallographic structures of **3**, **4**, **5b**, and **6a,b**; hydrogen atoms and solvent molecules are omitted for clarity. Ellipsoids drawn at 30% probability level.

diffusion of methanol to their chloroform solutions at room temperature (**3**, **4**, **6a**, **6b**) or at 0 °C (**5b**), though all efforts failed with **5a**. It is clear that **3** has a propargyl allenic structure via a head-to-tail dimerization process, while **4** and **5b** show a direct head-to-head linkage, consistent with the NMR and UV-vis absorption spectroscopic analyses. The distance linking the dimer is extremely long (1.605–1.610 Å) due to the steric repulsion between the two fluorenyl units. Interestingly, compounds **6a/6b** exhibit a unique difluorenylidene cyclobutene framework. The congested surroundings of the bulky mesityl and fluorenyl groups in **6a** makes a propeller-like, nonplanar conformation for the molecule, and a twist angle of about 5.8° is observed for the four-membered ring. This angle is further enlarged to be ~13.9° in **6b** due to the even more severe steric repulsion.

The as-formed dimers **5a/5b** seem to be only metastable, leading to a highly contorted difluorenylidene cyclobutene structure in high yield which was rarely reported.⁸ The formation of the cyclobutene quinodimethane moiety directly from the dialkyl intermediates poses a challenging mechanistic problem, and thus, a thermally induced rearrangement process⁹ may be involved (Scheme 2). The situation, generating a tail-to-

Scheme 2. Proposed Mechanism for the Formation of **6a/6b**



tail linked diallene-like structure **A**, becomes more reasonable. To monitor the speculated rearrangement intermediate, the time-dependent ¹³C NMR spectra (Figure S2) were recorded in CDCl₃. The characteristic allene peak could be observed at a chemical shift of 206 ppm after standing for 34 h at room temperature, indicating a probable conversation from the bis-propargyl to the diallenic intermediate in solution. Like most cyclobutenes promoted by 1,2-addition of allenic derivative itself,¹⁰ the proposed diallene **A** can undergo intramolecular rotation and then accomplish intramolecular electrocyclization¹¹ to give the final difluorenylidene cyclobutene products **6a/6b**. For intermediates **5a/5b**, they are stable enough for separation presumably due to their rigid conformation, which restrains molecular motion, especially in the solid state. It should be noted that thermal conversion of the propargyl allene (prepared from bromoallene) into the diallene structure was previously reported, and subsequent electrocyclization to cyclobutene can only be achieved by using transition-metal catalyst.⁸ Our new approach toward difluorenylidene cyclobutene derivatives using the dimerization of 9-ethynylfluorenyl radical followed by rearrangement and ring-cyclization is obviously more convenient and efficient.

To better understand the chemical reactivity of radical species EFR, the optimized geometric structures and the spin density distributions were calculated at the UB3LYP/6-31G (d, p) level (Figure 4). The spin densities at the *a*, *b*, *c* positions (Figure 1) of the fluorenyl moiety are in the range of 0.095–0.137 (Table 1), indicating that the two benzenoid rings largely share the electron-spin density over the cyclopentadienyl backbone. This result agrees well with our initial intention to

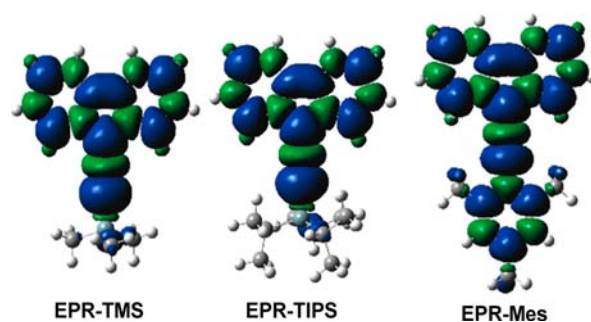


Figure 4. Spin-density distribution maps of EFRs with different substituents.

Table 1. Carbon Spin Densities Calculated at the UB3LYP/6-31G (d, p) Level

| site | EFR-TMS | EFR-TIPS | EFR-Mes |
|------|---------|----------|---------|
| a | 0.103 | 0.103 | 0.095 |
| b | 0.139 | 0.139 | 0.125 |
| c | 0.144 | 0.143 | 0.123 |
| d | 0.546 | 0.546 | 0.500 |
| e | 0.358 | 0.347 | 0.326 |

decrease the spin density on the head of the fulvenallenyl radical. The *d*, *e* positions of EPR have the largest amplitudes of 0.500–0.547 and 0.326–0.352, respectively. The ratios between the *d/e* positions are 1.53 for EFR-TMS and 1.57 for EFR-TIPS, respectively. This implies that the head *d* site of EFR-TIPS is more reactive than that of EFR-TMS. In addition, compared to the TMS group, the larger TIPS group greatly blocks the reactive *e* site in the allenic form, and thus both effects account for their different dimerization processes. The attachment of the bulky mesityl group to the tail of the 9-ethynylfluorenyl moiety leads to spin delocalization even extended to the mesityl group. The ratio between *d/e* positions of EFR-Mes is similar to that of EPR-TMS, but the steric overcrowding resultant from mesityl group facilitates the formation of the dipropinyl products. These results suggest that the different dimeric products result from the combined effect of both the spin distribution and steric hindrance.

In summary, we observed regioselective dimerization and subsequent ring cyclization processes of a series of substituted 9-ethynylfluorenyl radicals. Our structural and spectroscopic characterizations revealed that the TMS end-capped substrate featured a head-to-tail dimerization process, while the bulkier groups such as TIPS- and Mes-substituted analogues preferred a head-to-head homocoupling, which can be explained by their different spin distribution and steric hindrance effect. Moreover, it was also found that the Mes-substituted EFR dimeric can undergo rearrangement and ring-cyclization reaction at room temperature, eventually leading to the formation of the unique difluorenylidene cyclobutene structure in high yield. Our studies demonstrated the rich chemistry of reactive radical species and the possible formation of unique structures which cannot be approached easily by ordinary chemistry.

■ ASSOCIATED CONTENT

Supporting Information

The Supporting Information is available free of charge on the ACS Publications website at DOI: 10.1021/acs.orglett.6b02904.

Experimental details; NMR and mass spectra; single-crystal data for **3**, **4**, **5b**, and **6a,b** (PDF)

AUTHOR INFORMATION

Corresponding Author

*E-mail: zbzeng@hnu.edu.cn.

ORCID

Zebing Zeng: 0000-0002-9788-1988

Notes

The authors declare no competing financial interest.

ACKNOWLEDGMENTS

We thank the National Natural Science Foundation of China (21502049 and 51573040), start-up funding from Hunan University (531109020043), the opening fund of Hunan Normal University (Key Laboratory of Chemical Biology and Traditional Chinese Medicine Research, Ministry of Education of China), and the Singapore MOE Tier 3 programme (MOE2014-T3-1-004) for financial support.

REFERENCES

- (1) (a) Rajca, A. *Chem. Rev.* **1994**, *94*, 871. (b) Zhang, H.-R.; Wang, K. K. *J. Org. Chem.* **1999**, *64*, 7996. (c) Harrington, L. E.; Britten, J. F.; McGlinchey, M. J. *Org. Lett.* **2004**, *6*, 787. (d) Servais, A.; Azzouz, M.; Lopes, D.; Courillon, C.; Malacria, M. *Angew. Chem., Int. Ed.* **2007**, *46*, 576. (e) Yamada, M.; Akasaka, T.; Nagase, S. *Chem. Rev.* **2013**, *113*, 7209. (f) Sun, Z.; Zeng, Z.; Wu, J. *Acc. Chem. Res.* **2014**, *47*, 2582. (g) Zeng, Z.; Shi, X.; Chi, C.; Lopez Navarrete, J. T.; Casado, J.; Wu, J. *Chem. Soc. Rev.* **2015**, *44*, 6578. (h) Fu, X.; Zhao, D. *Org. Lett.* **2015**, *17*, 5694.
- (2) (a) Zhang, T.; Zhang, L.; Hong, X.; Zhang, K.; Qi, F.; Law, C. K.; Ye, T.; Zhao, P.; Chen, Y. *Combust. Flame* **2009**, *156*, 2071. (b) Steinbauer, M.; Hemberger, P.; Fischer, I.; Bodi, A. *ChemPhysChem* **2011**, *12*, 1795. (c) Giegerich, J.; Fischer, I. *Phys. Chem. Chem. Phys.* **2013**, *15*, 13162. (d) Chakraborty, A.; Fulara, J.; Maier, J. P. *Angew. Chem., Int. Ed.* **2016**, *55*, 228.
- (3) (a) da Silva, G.; Bozzelli, J. W. *J. Phys. Chem. A* **2009**, *113*, 12045. (b) da Silva, G.; Bozzelli, J. W. *J. Phys. Chem. A* **2009**, *113*, 8971. (c) Polino, D.; Famulari, A.; Cavallotti, C. *J. Phys. Chem. A* **2011**, *115*, 7928.
- (4) (a) Zeng, Z.; Sung, Y. M.; Bao, N.; Tan, D.; Lee, R.; Zafra, J. L.; Lee, B. S.; Ishida, M.; Ding, J.; López Navarrete, J. T.; Li, Y.; Zeng, W.; Kim, D.; Huang, K.-W.; Webster, R. D.; Casado, J.; Wu, J. *J. Am. Chem. Soc.* **2012**, *134*, 14513. (b) Tian, Y.; Uchida, K.; Kurata, H.; Hirao, Y.; Nishiuchi, T.; Kubo, T. *J. Am. Chem. Soc.* **2014**, *136*, 12784.
- (5) (a) Miller, J. A.; Klippenstein, S. J. *J. Phys. Chem. A* **2003**, *107*, 7783. (b) Hansen, N.; Kasper, T.; Klippenstein, S. J.; Westmoreland, P. R.; Law, M. E.; Taatjes, C. A.; Kohse-Hoinghaus, K.; Wang, J.; Cool, T. A. *J. Phys. Chem. A* **2007**, *111*, 4081.
- (6) Naoe, S.; Yoshida, Y.; Oishi, S.; Fujii, N.; Ohno, H. *J. Org. Chem.* **2016**, *81*, 5690.
- (7) Banide, E. V.; Molloy, B. C.; Ortin, Y.; Müller-Bunz, H.; McGlinchey, M. J. *Eur. J. Org. Chem.* **2007**, 2007, 2611.
- (8) (a) Pasto, D. J.; Mitra, D. K. *J. Org. Chem.* **1982**, *47*, 1381. (b) Oulié, P.; Altes, L.; Milosevic, S.; Bouteille, R.; Müller-Bunz, H.; McGlinchey, M. J. *Organometallics* **2010**, *29*, 676.
- (9) Skattebol, L.; Solomon, S. *J. Am. Chem. Soc.* **1965**, *87*, 4506.
- (10) Vogel, E. *Angew. Chem.* **1960**, *72*, 4. (b) Roberts, J. D.; Sharts, C. *M. Org. React.* **1962**, *12*, 1.
- (11) (a) Dolbier, W. R.; Koroniak, H.; Houk, K. N.; Sheu, C. *Acc. Chem. Res.* **1996**, *29*, 471. (b) Sakai, S. *J. Phys. Chem. A* **2006**, *110*, 9443.